JOURNAL OF MATERIALS SCIENCE 27 (1992) 1589–1598

Analysis of elastic interactions between holes

K. DAVANAS
Ministry of Defence, Tassopoulou 14, Agia Paraskevi, Athens 15342, Greece

The elastic interactions between holes, i.e. pressurized, equilibrium and underpressurized bubbles or cavities, are analysed. By using rigorous mathematical methods, exact and easy-to-use formulae are derived for the description of the interactions. It is proven that, contrary to previous understanding, all elastic interactions between holes are repulsive. The magnitude of the repulsive force is found to increase for decreasing hole-to-hole separations. Thus bubble coalescence can be severely inhibited, which among other effects can lead to lower material swelling. Finally, the possible role of elastic repulsions in explaining the stability of the commonly observed bubble lattices is discussed.

1. Introduction

Elastic interactions between holes are of great importance in connection with material swelling and bubble lattice formation. The strong interest in these phenomena, especially in the nuclear industry, is reflected in the extensive experimental and theoretical work [1–6] that has been done to date. However, the theoretical models that have appeared in the literature use approximations rather than an exact description of the elastic field which determines the interactions. Consequently, agreement with experiments is not always obvious. So, for instance, the apparent repulsion between small overpressurized and large equilibrium bubbles observed in the experiments by Barnes and Mazey [1] is not easily reconciled with model predictions which dictate that all bubbles, regardless of their pressure (or, in general, surface traction) attract each other. In addition, the stability of bubble lattices commonly observed in irradiated metals [7–9] is difficult to explain under this assumption of universal attraction among bubbles.

In the present study, a mathematically rigorous and exact solution of the elasticity equations pertaining to interacting holes is provided; thus, the nature of the interaction (attractive or repulsive) as well as its magnitude, is determined unambiguously. Closed-form solutions are obtained for the interaction between two equi-sized and equi-pressurized holes; between one pressurized and one equilibrium hole of equal size; between a small pressurized and a large equilibrium hole; and between two equi-sized holes with surface tractions equal in magnitude but opposite in sign (i.e. one pressurized and one with tensile traction on its surface). The last case pertains to cavities which exert a tensile stress on the surrounding matrix due to their surface tension. The results show that, contrary to previous beliefs, the elastic interaction between holes, regardless of their surface traction, is repulsive.

2. General equations

To find the elastic interaction between two holes in an infinite isotropic medium, the total elastic energy E_{tot} has to be known. Then, the elastic interaction force F_{el} will be given by

$$F_{el} = -\frac{\partial E_{tot}}{\partial L} \tag{1}$$

where L is the separation distance between the holes (i.e. tip-to-tip).

The holes are modelled as two infinitely long cylinders; this does not alter the nature (attractive or repulsive) of the interaction nor does it make any significant difference quantitatively, since energies and stress concentrations calculated for spheres or cylinders differ only by small numerical factors, if at all. For example, the total elastic energy of an isolated pressurized sphere and the elastic energy of an isolated pressurized cylinder are given by virtually identical expressions [10, 11]. In the classical elasticity problems of a sphere or hole subjected to an applied stress at infinity, one finds again that the stress concentrations at the peripheries of the sphere or the hole differ only by a small (=0.75) numerical factor [10–12]. The same is true when one compares the stress concentrations of two neighbouring spheres to those of two neighbouring cylinders [12, 13].

Bipolar co-ordinates are especially suitable for modelling a pair of inifinitely long holes in an infinite medium. The equations of transformation between cartesian (x, y, z) and bipolar (η, ξ, z') co-ordinates are [10, 11, 14]

$$\begin{aligned} x &= \frac{J \mathrm{sh}\eta}{\mathrm{ch}\eta - \cos\xi} \\ y &= \frac{J \sin\xi}{\mathrm{ch}\eta - \cos\xi} \\ z &= z' \end{aligned} \tag{2}$$

where J is the Jacobian of the transformation given by [10, 11, 14]

$$J = \frac{a}{\mathrm{ch}\eta - \cos\xi} \tag{3}$$

and a is a parameter dependent on the radii of the holes and the distance between them as follows.

Equation 2 defines an infinite number of circles in the (x, y) plane, given by the relations

$$(x - a\coth)^2 + y^2 = \frac{a^2}{\mathrm{sh}^2\eta}$$
$$(y - a\cot\xi)^2 + x^2 = \frac{a^2}{\sin^2\xi} \quad (4)$$

Assume that the infinitely long cylinders occupy the circles η_1 and η_2 (see Fig. 1). When both holes have the same radius $R_1 = R_2 = R$, then their positions are symmetrical

$$-\eta_2 = \eta_1 = \eta_0 > 0 \quad (5)$$

with

$$a = R\,\mathrm{sh}\eta_1 = -R\,\mathrm{sh}\eta_2 = R\,\mathrm{sh}\eta_0 \quad (6)$$

and

$$a^2 = \left(\frac{L}{2} + R\right)^2 - R^2 \quad (7)$$

To solve for the elastic field under any boundary conditions at η_1, η_2 (i.e. under any applied stresses at the surfaces of the holes), the appropriate Airy stress function Φ has to be determined. This is given as a solution [10] of the well-known biharmonic equation

$$\nabla^4\Phi = 0 \quad (8)$$

In bipolar co-ordinates, Equation 8 takes the form [14]

$$\left[\frac{\partial^4}{\partial\xi^4} + 2\frac{\partial^4}{\partial\xi^2\partial\eta^2} + \frac{\partial^4}{\partial\eta^4} + 2\frac{\partial^2}{\partial\xi^2} - 2\frac{\partial^2}{\partial\eta^2} + 1\right]\frac{\Phi}{J} = 0 \quad (9)$$

Once Φ is known, the stresses can be obtained from [14]

$$a\sigma_\eta = \left[(\mathrm{ch}\eta - \cos\xi)\frac{\partial^2}{\partial\xi^2} - \mathrm{sh}\eta\frac{\partial}{\partial\eta} - \sin\xi\frac{\partial}{\partial\xi} + \mathrm{ch}\eta\right]\frac{\Phi}{J} \quad (10)$$

$$a\sigma_\xi = \left[(\mathrm{ch}\eta - \cos\xi)\frac{\partial^2}{\partial\eta^2} - \mathrm{sh}\eta\frac{\partial}{\partial\eta} - \sin\xi\frac{\partial}{\partial\xi} + \cos\xi\right]\frac{\Phi}{J} \quad (11)$$

$$a\sigma_{\eta\xi} = -(\mathrm{ch}\eta - \cos\xi)\frac{\partial^2(\Phi/J)}{\partial\eta\partial\xi} \quad (12)$$

where ε represents strains.
Hooke's Law takes the form

$$\sigma_\eta = \lambda(\varepsilon_\eta + \varepsilon_\xi) + 2G\varepsilon_\eta$$
$$\sigma_\xi = \lambda(\varepsilon_\eta + \varepsilon_\xi) + 2G\varepsilon_\xi \quad (13)$$
$$\sigma_{\eta\xi} = 2G\varepsilon_{\eta\xi}$$

where G is the shear modulus, λ the Lame constant $= \nu E/(1 + \nu)(1 - 2\nu)$, with E the Young's modulus, and ν Poisson's ratio.

The next step is to determine the displacements u (in the η direction) and v (in the ξ direction); these are

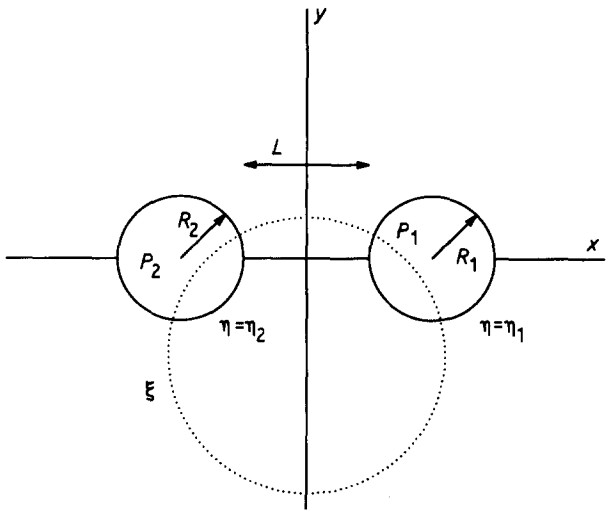

Figure 1 Representation of holes by the use of bipolar co-ordinates.

given by [11]

$$\varepsilon_\eta = \frac{1}{J}\frac{\partial u}{\partial\eta} - v\frac{\partial(1/J)}{\partial\xi}$$
$$\varepsilon_\xi = \frac{1}{J}\frac{\partial v}{\partial\xi} - u\frac{\partial(1/J)}{\partial\eta} \quad (14)$$
$$\varepsilon_{\eta\xi} = \frac{\partial}{\partial\eta}\frac{v}{J} + \frac{\partial}{\partial\xi}\frac{u}{J}$$

Equations 9–14 can be combined to yield the displacements in terms of Φ explicitly [15].

$$2Gu = \frac{G}{\lambda + G}\frac{1}{J}\frac{\partial\Phi}{\partial\eta} - \frac{1}{J}\frac{\partial\Lambda}{\partial\xi} \quad (15)$$

$$2Gv = \frac{G}{\lambda + G}\frac{1}{J}\frac{\partial\Phi}{\partial\xi} + \frac{1}{J}\frac{\partial\Lambda}{\partial\eta} \quad (16)$$

where

$$\frac{\Lambda}{J} = \frac{\lambda + 2G}{2(\lambda + G)}\iint\left[\frac{\partial^2}{\partial\eta^2} - \frac{\partial^2}{\partial\xi^2} - 1\right]\frac{\Phi}{J}\,d\eta\,d\xi \quad (17)$$

The total elastic energy of the system can be found from

$$E_{\mathrm{tot}} = \frac{1}{2}\int_{\mathrm{SUR}} -P_1'u(\eta_1)\,dS + \frac{1}{2}\int_{\mathrm{SUR}} -P_2'u(\eta_2)\,dS \quad (18)$$

where P_i' is the gas pressure in hole i ($i = 1,2$) and the integrals are taken over the surface of each hole.

In order exactly to determine the interaction between the two holes, one also needs to account for the effect of the surface energies of the holes. It has been shown [5] that this is done by substituting in Equation 10 the uncompensated pressures $P_i = P_i' - 2\gamma/R_i$ in place of the actual gas pressures in the holes, i.e

$$E_{\mathrm{tot}} = \frac{1}{2}\int_{\mathrm{SUR}} -P_1u(\eta_1)\,dS + \frac{1}{2}\int_{\mathrm{SUR}} -P_2u(\eta_2)\,dS \quad (20)$$

where γ is the surface energy.

Finally, using Equation 20, the sign and magnitude of the interaction force between holes is obtained.

Note that the above analysis pertains to plane-strain elasticity problems. The holes can be pressurized, equilibrated, or even exert a tensile stress on the surroundings (if $P_i' = 0$, then $P_i = -2\gamma/R_i < 0$). In solving for the stress function Φ, the state of the holes is incorporated by the use of appropriate boundary conditions. Specific cases are studied in the next section.

3. Results

As mentioned in the Introduction, the following four cases will be examined in detail: (I) two equi-sized and equi-pressurized holes; (II) two equi-sized holes, one pressurized and one equilibrium; (III) one small pressurized and one large equilibrium hole; (IV) two equi-sized holes with surface tractions equal but of opposite sign.

3.1. Case I: $R_1 = R_2$, $P_1 = P_2$

The two holes are at symmetrical positions $\eta_1 = \eta_0 = -\eta_2$ ($\eta_0 > 0$), where η's are given by Equations 5–7 as a function of the common radius R and the separation distance L. The appropriate boundary conditions are

$$\sigma_\eta(\eta = \eta_1) = -P_1, \quad \sigma_\eta(\eta = \eta_2) = -P_2,$$
$$\sigma_{\eta\xi}(\eta_1) = \sigma_{\eta\xi}(\eta_2) = 0 \tag{21}$$

where $P = P_1 = P_2$ and

$$\sigma_\eta(\infty) = \sigma_\xi(\infty) = \sigma_{\eta\xi}(\infty) = 0 \tag{22}$$

Thus, the biharmonic Equation 9 has to be solved along with the boundary conditions in Equations 21 and 22. The appropriate stress function Φ which fulfills all the above requirements is

$$\frac{\Phi}{J} = K(\mathrm{ch}\eta - \cos\xi)\ln(\mathrm{ch}\eta - \cos\xi) + \sum_{n=1}^{\infty} \cos n\xi\,[A_n \mathrm{ch}(n+1)\eta + B_n \mathrm{ch}(n-1)\eta] \tag{23}$$

where K, A_n and B_n are constants. These constants can be derived from the work of Ling [14], where the problem of two holes under stress at infinity is solved. To satisfy the boundary condition of equal pressures at the hole surfaces, Equations 10–12 are solved simultaneously to yield

$$A_n = \frac{2K(e^{-n\eta_0}\mathrm{sh}n\eta_0 + ne^{-\eta_0}\mathrm{sh}\eta_0)}{n(n+1)(\mathrm{sh}2n\eta_0 + n\mathrm{sh}2\eta_0)},$$
$$B_n = \frac{2K(e^{-n\eta_0}\mathrm{sh}n\eta_0 + ne^{\eta_0}\mathrm{sh}\eta_0)}{n(n-1)(\mathrm{sh}2n\eta_0 + n\mathrm{sh}2\eta_0)} \tag{24}$$

except

$$B_1 = \frac{1}{2}(K\mathrm{th}\eta_0 \mathrm{ch}2\eta_0 - 2aP_0) \tag{25}$$

where P_0 is a parameter having the dimensions of pressure; for the present case I, $P_0 = P$. In case II though, P_0 is smaller than P, as will be seen later.

Equation 22 of zero stresses at infinity requires

$$\frac{\Phi}{J} \to 0 \quad \text{for} \quad \eta, \xi \to 0 \tag{26}$$

Applying Equation 26 to Equation 23, one finds

$$\sum_{n=1}^{\infty}(A_n + B_n) = 0 \tag{27}$$

Substituting Equations 24 and 25 into Equation 27 and solving for K

$$\frac{K}{aP_0} = \left[\frac{1}{2} + \mathrm{th}\eta_0 \mathrm{sh}^2\eta_0 - 4\sum_{n=2}^{\infty}\frac{e^{-n\eta_0}\mathrm{sh}n\eta_0 + n\mathrm{sh}\eta_0(n\mathrm{sh}\eta_0 + \mathrm{ch}\eta_0)}{n(n^2-1)(\mathrm{sh}2n\eta_0 + n\mathrm{sh}2\eta_0)}\right]^{-1} \tag{28}$$

The next step is to calculate Λ of Equations 15–17 in order to find the displacements. Substituting the expression for Φ/J from Equation 23 into 17 and carrying out the integration yields

$$\frac{\Lambda}{J}\frac{2(\lambda+G)}{aP(\lambda+2G)} = 2\xi\mathrm{sh}\eta - 2\sin\xi + \frac{2(e^\eta+1)^2}{e^\eta} \times \arctan\frac{\sin\xi(1+e^\eta)}{(e^\eta-1)(1+\cos\xi)} - \frac{2(e^{2\eta}+2e^\eta-1)}{e^\eta}\arctan\frac{\sin\xi}{1+\cos\xi} + 4(1+\cos\xi)\arctan\frac{e^\eta-\cos\xi}{\sin\xi} + \frac{2}{aP}\sum_{n=1}^{\infty}\left[A_n\mathrm{sh}(n+1)\eta\sin n\xi + B_n\mathrm{sh}(n-1)\eta\sin n\xi\right] \tag{29}$$

Knowing Λ and Φ, the displacements can be found from Equations 15 and 16. So the displacement along the η direction is obtained from

$$u = \frac{1}{2(\lambda+G)}\left[\frac{\partial(\Phi/J)}{\partial\eta} - \frac{\mathrm{sh}\eta}{\mathrm{ch}\eta - \cos\xi}\frac{\Phi}{J}\right] + \frac{1}{2G}\left[\frac{\sin\xi}{\mathrm{ch}\eta - \cos\xi}\frac{\Lambda}{J} - \frac{\partial(\Lambda/J)}{\partial\xi}\right] \tag{30}$$

where Φ/J and Λ/J are given by Equations 23 and 29.

Taking the integral as indicated in Equation 20, the energy of the system is obtained. Due to symmetry, Equation 20 is equivalent to

$$E_{\mathrm{tot}} = \int_{\mathrm{SUR}} -Pu(\eta_0)\,\mathrm{d}S \tag{31}$$

The integration is carried over the surface of the hole (i.e. at $\eta = \eta_1 = \eta_0$); thus

$$\mathrm{d}S = J\,\mathrm{d}\xi = \frac{a\,\mathrm{d}\xi}{\mathrm{ch}\eta_0 - \cos\xi} \tag{32}$$

Combining Equations 30–32

$$2GE_{\mathrm{tot}} = \frac{-PG}{\lambda+G}\int_{-\pi}^{\pi}\left.\frac{\partial\Phi}{\partial\eta}\right|_{\eta_0}\mathrm{d}\xi + P[\Lambda(\eta_0,\pi) - \Lambda(\eta_0,-\pi)] \tag{33}$$

From Equation 23 one finds

$$\int_{-\pi}^{\pi} \left.\frac{\partial\Phi}{\partial\eta}\right|_{\eta_0} d\xi = 2\pi aK + 8\pi aA_1 \operatorname{ch}\eta_0 e^{-\eta_0} - \frac{2\pi aA_1 \operatorname{ch}2\eta_0}{\operatorname{sh}^2\eta_0} - \frac{2\pi aB_1}{\operatorname{sh}^2\eta_0} + \frac{2\pi a}{\operatorname{sh}\eta_0}\sum_{n=2}^{\infty} e^{-n\eta_0} \times [(n+1)A_n \operatorname{sh}(n+1)\eta_0 + (n-1)B_n \operatorname{sh}(n-1)\eta_0] - \frac{2\pi a}{\operatorname{sh}^2\eta_0}\sum_{n=2}^{\infty} e^{-n\eta_0}(n\operatorname{sh}\eta_0 + \operatorname{ch}\eta_0)[A_n \operatorname{ch}(n+1)\eta_0 + B_n \operatorname{ch}(n-1)\eta_0]$$

After some algebra the above equation becomes

$$\int_{-\pi}^{\pi} \left.\frac{\partial\Phi}{\partial\eta}\right|_{\eta_0} d\xi = 2\pi aK + 8\pi aA_1 \operatorname{ch}\eta_0 e^{-\eta_0} - \frac{2\pi aA_1 \operatorname{ch}2\eta_0}{\operatorname{sh}^2\eta_0} - \frac{2\pi aB_1}{\operatorname{sh}^2\eta_0} - \frac{4\pi aK}{\operatorname{sh}^2\eta_0} S_0 \qquad (34)$$

where

$$S_0 = \sum_{n=2}^{\infty} \frac{(n-1)(e^{-n\eta_0}\operatorname{sh}n\eta_0 + ne^{-\eta_0}\operatorname{sh}\eta_0)[\operatorname{ch}n\eta_0 + n\operatorname{sh}\eta_0 e^{-(n+1)\eta_0}] - (n+1)(e^{-n\eta_0}\operatorname{sh}n\eta_0 + ne^{\eta_0}\operatorname{sh}\eta_0)[n\operatorname{sh}\eta_0 e^{-(n-1)\eta_0} - \operatorname{ch}n\eta_0]}{e^{n\eta_0} n(n^2-1)(\operatorname{sh}2n\eta_0 + n\operatorname{sh}2\eta_0)} \qquad (35)$$

From Equation 29 one finds

$$\Lambda(\eta_0, \pi) - \Lambda(\eta_0, -\pi) = \frac{\lambda + 2G}{(\lambda + G)} \frac{\pi a^2 P}{1 + \operatorname{ch}\eta_0} \times \left[2\operatorname{sh}\eta_0 + \frac{(e^{\eta_0}+1)^2}{e^{\eta_0}} - \frac{e^{2\eta_0} + 2e^{\eta_0} - 1}{e^{\eta_0}}\right] \qquad (36)$$

Therefore, Equation 33 for the total energy becomes

$$E_{\text{tot}} = \frac{-P}{2(\lambda + G)}\left[2\pi aK + 4\pi aKe^{-2\eta_0} - \frac{\pi aK \operatorname{ch}2\eta_0 e^{-\eta_0}}{\operatorname{sh}^2\eta_0 \operatorname{ch}\eta_0} + \frac{2\pi a^2 P}{\operatorname{sh}^2\eta_0} - \frac{2\pi aK \operatorname{ch}2\eta_0}{\operatorname{sh}2\eta_0} - \frac{4\pi aK}{\operatorname{sh}^2\eta_0} S_0\right] + \frac{\pi aKP}{1 + \operatorname{ch}\eta_0} \frac{\lambda + 2G}{G(\lambda + G)} (\operatorname{sh}\eta_0 + e^{-\eta_0}) \qquad (37)$$

The above expression has all the information about the hole-to-hole interaction. However, it is not easy to use because it contains K and S_0 which are given in terms of infinite series as seen from Equations 28 and 35. The behaviour and the sums of these infinite series need to be studied in detail, because they will reveal the functional dependencies of E_{tot}.

As seen from Equations 5–7, the limiting case $\eta_0 \to \infty$ ($L/R \gg 1$) corresponds to two separate (isolated) holes; under these circumstances the interaction is expected to be virtually zero, i.e. the total energy should be found equal to the energy of an isolated (pressurized) hole multiplied by 2. The limiting case $\eta_0 \to 0$ ($L/R \to 0$) will reveal what happens to the total energy as the two holes approach each other, an increase in E_{tot} as $\eta_0 \to 0$ will mean repulsion, and a decrease will mean attraction.

Let us first find the sum of the series in Equation 28 for various limiting cases. Dividing both numerator and denominator by $\operatorname{sh}2n\eta_0$, one obtains

$$\sum_{n=2}^{\infty} \frac{e^{-n\eta_0}\operatorname{sh}n\eta_0 + n\operatorname{sh}\eta_0(n\operatorname{sh}\eta_0 + \operatorname{ch}\eta_0)}{n(n^2-1)(\operatorname{sh}2n\eta_0 + n\operatorname{sh}2\eta_0)} = \sum_{n=2}^{\infty} \frac{e^{-n\eta_0}\dfrac{\operatorname{sh}n\eta_0}{\operatorname{sh}2n\eta_0} + \dfrac{n^2\operatorname{sh}^2\eta_0}{\operatorname{sh}2n\eta_0} + \dfrac{n\operatorname{sh}2\eta_0}{\operatorname{sh}2n\eta_0}}{n(n^2-1)\left(1 + \dfrac{n\operatorname{sh}2\eta_0}{\operatorname{sh}2n\eta_0}\right)} \qquad (38)$$

For $\eta_0 \to \infty$, $\operatorname{th}\eta_0 \to 1$ and

$$\frac{n\operatorname{sh}\eta_0}{\operatorname{sh}n\eta_0} \cong \frac{ne^{\eta_0}/2}{e^{n\eta_0}/2} = \frac{n}{e^{(n-1)\eta_0}}$$

$$= \frac{n}{1 + (n-1)\eta_0 + \frac{1}{2}(n-1)^2\eta_0^2 + \ldots} \to 0$$

Thus, the infinite series of Equation 38 approaches zero. Since $\eta_0 \gg 1$ for $\eta_0 \to \infty$, Equation 28 yields

$$K \to \frac{aP_0}{\operatorname{sh}^2\eta_0} \qquad (39)$$

On the other hand, for $\eta_0 \to 0$, $\operatorname{sh}\eta_0 \to \eta_0$ and $\operatorname{ch}\eta_0 \to 1$ and $e^{\eta_0} \to 1$. Under these circumstances Ling [14] has shown that

$$K \to \frac{10}{7} \frac{aP_0}{\operatorname{sh}^2\eta_0} \qquad (40)$$

Let us now find the sum of the infinite series in Equation 35; dividing both numerator and denominator by $\operatorname{sh}2n\eta_0$ one obtains

$$S_0 = \sum_{n=2}^{\infty} \frac{(n-1)\left(\dfrac{\operatorname{sh}n\eta_0}{e^{n\eta_0}\operatorname{sh}2n\eta_0} + \dfrac{ne^{-\eta_0}\operatorname{sh}\eta_0}{\operatorname{sh}2n\eta_0}\right)\left[\dfrac{\operatorname{ch}n\eta_0}{e^{n\eta_0}} + \dfrac{n\operatorname{sh}\eta_0}{e^{(2n+1)\eta_0}} + \dfrac{n\operatorname{sh}\eta_0}{e^{(2n+1)\eta_0}}\right] - (n+1)\left(\dfrac{\operatorname{sh}n\eta_0}{e^{n\eta_0}\operatorname{sh}2n\eta_0} + \dfrac{ne^{\eta_0}\operatorname{sh}\eta_0}{\operatorname{sh}2n\eta_0}\right)\left[\dfrac{n\operatorname{sh}n\eta_0}{e^{(2n-1)\eta_0}} - \dfrac{\operatorname{ch}n\eta_0}{e^{n\eta_0}}\right]}{n(n^2-1)\left(1 + \dfrac{n\operatorname{sh}2\eta_0}{\operatorname{sh}2n\eta_0}\right)} \qquad (41)$$

For $\eta_0 \to \infty$, the numerator approaches zero while the denominator remains finite, thus

$$S_0 \to 0 \qquad (42)$$

On the other hand, for $\eta_0 \to 0$, $\operatorname{sh}\eta_0 \to \eta_0$ and $\operatorname{ch}\eta_0 \to 1$ and $e^{\eta_0} \to 1$; thus

$$\sum_{n=2}^{\infty}\frac{(n-1)(e^{-n\eta_0}\mathrm{sh}n\eta_0+ne^{-\eta_0}\mathrm{sh}\eta_0)\,[\mathrm{ch}n\eta_0+n\mathrm{sh}\eta_0 e^{-(n+1)\eta_0}]-(n+1)(e^{-n\eta_0}\mathrm{sh}n\eta_0+ne^{\eta_0}\mathrm{sh}\eta_0)\,[n\mathrm{sh}\eta_0 e^{-(n-1)\eta_0}-\mathrm{ch}n\eta_0]}{e^{n\eta_0}n(n^2-1)(\mathrm{sh}2n\eta_0+n\mathrm{sh}2\eta_0)}$$

$$\leq\sum_{n=2}^{\infty}\frac{(e^{-n\eta_0}\mathrm{sh}n\eta_0+ne^{\eta_0}\mathrm{sh}\eta_0)(2\mathrm{ch}n\eta_0)}{e^{n\eta_0}(n^2-1)(\mathrm{sh}2n\eta_0+n\mathrm{sh}2\eta_0)}=\sum_{n=2}^{\infty}\frac{e^{-n\eta_0}}{n^2-1}\frac{\mathrm{ch}n\eta_0(\mathrm{sh}2n\eta_0+2n\mathrm{sh}\eta_0)-\mathrm{sh}n\eta_0\mathrm{sh}2n\eta_0}{\mathrm{sh}2n\eta_0+n\mathrm{sh}2\eta_0}$$

$$=\sum_{n=2}^{\infty}\frac{e^{-n\eta_0}}{n^2-1}\left[\mathrm{ch}n\eta_0-\frac{\mathrm{sh}n\eta_0}{1+2n\mathrm{sh}\eta_0/\mathrm{sh}2n\eta_0}\right]\leq\sum_{n=2}^{\infty}\frac{e^{-n\eta_0}}{n^2-1}\left[\mathrm{ch}n\eta_0-\frac{\mathrm{sh}n\eta_0}{2}\right]$$

$$=\sum_{n=2}^{\infty}\frac{1}{n^2-1}\left[\frac{1}{4}+\frac{3}{4}e^{2n\eta_0}\right]\leq\sum_{n=2}^{\infty}\frac{1}{n^2-1}=\frac{3}{4}$$

where the equal signs apply for η_0 equal to zero. Hence, for $\eta_0 \to 0$

$$S_0 \to \frac{3}{4} \tag{43}$$

Now, one can use Equation 37 in connection with the sums of K and S_0. Using $\lambda = 2G$ (i.e. $\nu = 1/3$, the standard value for Poisson's ratio), and taking the limit of E_{tot} from Equation 37 for $\eta_0 \to \infty$ ($K \to aP_0/\mathrm{sh}^2\eta_0$, $S_0 \to 0$, $\mathrm{th}\eta_0 \to 1$) one obtains after the algebra

$$E_{tot} = 2\frac{\pi P^2 R^2}{2G} = 2E_0 = E_\infty \tag{44}$$

where E_0 is the energy of a single (pressurized) hole [10], and $E_\infty = 2E_0$ is the energy of the system of two holes at infinite separation.

As seen from Equation 44 there is excellent agreement with reality, since the expression for the total energy yields, at large separations, the energy of one pressurized hole multiplied by 2.

Taking the limit of E_{tot} for $\eta_0 \to 0$ ($K \to 10aP_0/7\,\mathrm{sh}^2\eta_0$, $S_0 \to 3/4$, $\mathrm{ch}\eta_0 \to 1$, $\mathrm{sh}\eta_0 \to \eta_0$, $e^{\eta_0} \to 1$) one finds

$$E_{tot} = -\frac{8}{5}E_0 + \frac{10}{21}E_0\frac{1}{\eta_0} + 2E_0\frac{1}{\eta_0^2} \tag{45}$$

Since the above formula is valid for $\eta_0 \to 0$, the last term dominates, thus

$$E_{tot} = 2E_0\frac{1}{\eta_0^2} \tag{46}$$

For very small values of η_0

$$\eta_0 \cong \mathrm{sh}\eta_0 = \frac{a}{R} = \frac{[(R+L/2)^2 - R^2]^{1/2}}{R} \cong \left[\frac{L}{R}\right]^{1/2} \tag{47}$$

Therefore, Equation 46 becomes

$$E_{tot} = 2E_0\frac{R}{L} \tag{48}$$

A simple superposition of Equations 44 and 48 describes both the short range and the long range interaction

$$E_{tot} = 2E_0 + 2E_0\frac{R}{L} = E_\infty + E_\infty\frac{R}{L} \tag{49}$$

The result is plotted in Fig. 2. With the energy of the system increasing for approaching holes, the interaction force is obviously repulsive. The derivative of E_{tot} with respect to L yields the magnitude of the repulsive force F_{el}.

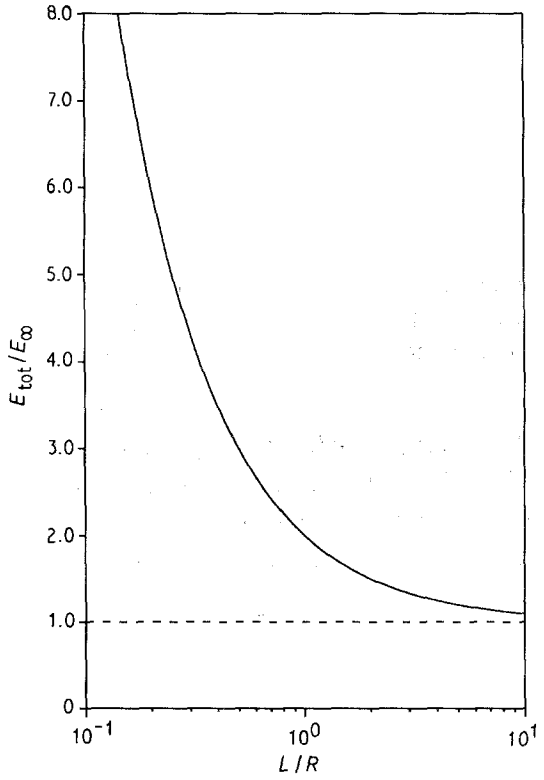

Figure 2 Ratio of the total energy E_{tot} of a system of two equi-sized and equi-pressurized holes over the energy E_∞ of two isolated holes with the same pressure and radius R, as a function of separation L.

It is interesting to compare F_{el} to other natural forces exerted on a bubble, as for instance, the retaining force of a grain boundary on a bubble F_{gb}, and the force of a dislocation on a bubble F_{dis}. The maximum values of these forces are given by [2]

$$F_{gb} = \pi R\gamma_{gb} \tag{50}$$

$$F_{dis} = Gb^2 \tag{51}$$

where γ_{gb} is the grain boundary energy, and b is Burger's vector. For typical bubbles in copper, i.e. with $R = 1\ \mu\mathrm{m}$, $P = 1\ \mathrm{MPa}$, $\gamma_{gb} = 0.654\ \mathrm{J\,m^{-2}}$, $E = 12.4 \times 10^{10}\ \mathrm{Pa}$, and $b = 2.56 \times 10^{-10}\ \mathrm{m}$, one finds

$$F_{gb} = 2 \times 10^{-6}\ \mathrm{Pa}, \quad F_{dis} = 3 \times 10^{-9}\ \mathrm{Pa} \tag{52}$$

The above forces pertain to spherical bubbles rather than infinitely long cylinders, as does $F_{el} = -\partial E_{tot}/\partial L$. To derive the F_{el} for spheres (so that similar things can be compared), the ratio E_{tot}/E_∞ is taken as being the same for a pair of spheres or a pair of cylinders; this is not expected to alter the results to

any considerable degree, if at all, in view of what has been said in the previous section. From Equation 49

$$\frac{E_{tot}}{E_\infty} = 1 + \frac{R}{L}$$

Therefore, in absolute terms

$$\frac{d(E_{tot}/E_\infty)}{dL} = \frac{R}{L^2}$$

or

$$\frac{dE_{tot}}{dL} = E_\infty \frac{R}{L^2} \quad (53)$$

For two spheres at infinite separation [10, 11]

$$E_\infty = 2\frac{\pi R^3 P^2}{2G} \quad (54)$$

Combining Equations 53 and 54

$$F_{el} = \left[\frac{R}{L}\right]^2 \frac{\pi P^2 R^2}{G} \quad (55)$$

The three forces F_{el}, F_{gb} and F_{dis} are compared in Fig. 3. Obviously, F_{el} far exceeds the other two in magnitude.

3.2. Case II: $R_1 = R_2$, $P_1 > P_2 = 0$

The biharmonic Equation 9 has to be solved along with the following boundary conditions:

$$\sigma_\eta(\eta_1 = \eta_0) = -P_1, \quad \sigma_\eta(\eta_2 = -\eta_0) = 0,$$
$$\sigma_{\eta\xi}(\eta_1) = \sigma_{\eta\xi}(\eta_2) = 0 \quad (56)$$

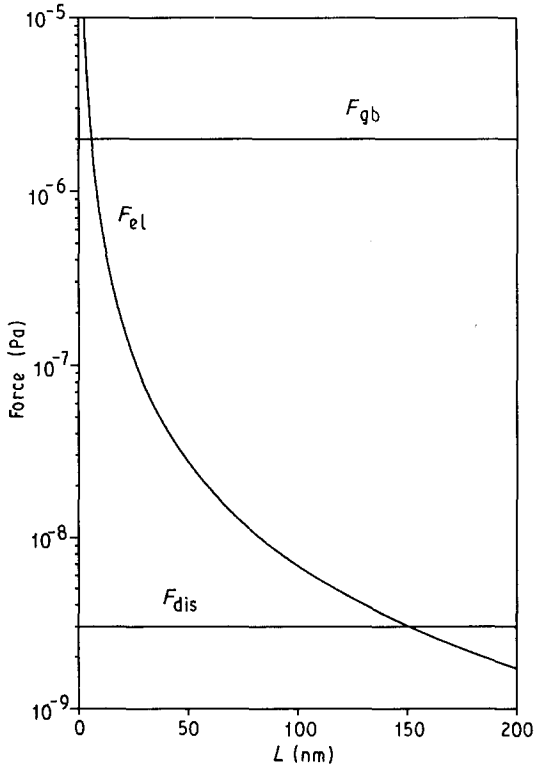

Figure 3 Comparison of forces exerted on a pressurized bubble by a neighbouring similar bubble F_{el}, by a grain boundary F_{gb}, and by a dislocation F_{dis}, as a function of separation L. $P = 1$ MPa; $R = 1$ μm.

where $P = P_1$, and

$$\frac{\Phi}{J} \to 0 \quad \text{for} \quad \eta, \xi \to 0$$

The last condition is equivalent to no stress at infinity. Note that $-\eta_2 = \eta_1 = \eta_0 > 0$, i.e. the holes occupy symmetric positions as in case I.

The appropriate stress function Φ fulfilling all the above requirements is

$$\begin{aligned}\frac{\Phi}{J} = {} & \frac{aP\eta \mathrm{ch}2\eta_0(\mathrm{ch}\eta - \cos\xi)}{\mathrm{sh}2\eta_0(\mathrm{ch}2\eta_0 - 1)} - \frac{aP\cos\xi}{4} \\ & + \frac{aP\,\mathrm{sh}2\eta\cos\xi}{2\mathrm{sh}2\eta_0(\mathrm{ch}2\eta_0 - 1)} + \frac{aP\,\mathrm{ch}\eta}{4} \\ & + K(\mathrm{ch}\eta - \cos\xi)\ln(\mathrm{ch}\eta - \cos\xi) \\ & + \sum_{n=1}^{\infty} \cos n\xi\,[A_n \mathrm{ch}(n+1)\eta \\ & + B_n \mathrm{ch}(n-1)\eta] \end{aligned} \quad (57)$$

The constants K, A_n and B_n are given by the same Equations 24, 25 and 28 as in case I; the only difference is that P_0 is now given by $P_0 = P/2$. Substituting the above expression for Φ into Equation 17 and working out the algebra

$$\begin{aligned}\frac{\Lambda}{J}\frac{4(\lambda+G)}{aP(\lambda+2G)} = {} & \frac{4\mathrm{ch}2\eta_0\mathrm{ch}\eta + 2\mathrm{ch}2\eta\cos\xi}{\mathrm{sh}2\eta_0(\mathrm{ch}2\eta_0 - 1)} \\ & + 2\xi\mathrm{sh}\eta - 2\sin\xi + \frac{2(e^\eta+1)^2}{e^\eta} \\ & \times \arctan\frac{\sin\xi(1+e^\eta)}{(e^\eta-1)(1+\cos\xi)} \\ & - \frac{2(e^{2\eta}+2e^\eta-1)}{e^\eta}\arctan\frac{\sin\xi}{1+\cos\xi} \\ & + 4(1+\cos\xi)\arctan\frac{e^\eta - \cos\xi}{\sin\xi} \\ & + \frac{4}{aP}\sum_{n=1}^{\infty}[A_n\mathrm{sh}(n+1)\eta\sin n\xi \\ & + B_n\mathrm{sh}(n-1)\eta\sin n\xi] \end{aligned} \quad (58)$$

From Equations 15, 16, 57 and 58 the displacements u, v and the total energy can be found. The latter is given by

$$\begin{aligned} GE_{tot} = {} & \frac{-PG}{\lambda+G}\int_{-\pi}^{\pi}\left.\frac{\partial\Phi}{\partial\eta}\right|_{\eta_0} d\xi \\ & + P[\Lambda(\eta_0,\pi) \\ & - \Lambda(\eta_0,-\pi)] \end{aligned} \quad (59)$$

Substituting for Φ and Λ in Equation 59 yields

$$\begin{aligned} E_{tot} = {} & -\frac{\pi a^2 P^2}{2(\lambda+G)\mathrm{sh}2\eta_0(\mathrm{ch}2\eta_0-1)} \\ & \left[\mathrm{ch}2\eta_0 + \frac{\mathrm{ch}2\eta_0 e^{-\eta_0}}{\mathrm{sh}\eta_0} - \frac{1}{\mathrm{th}\eta_0}\right] - \frac{\pi aPK(1+2e^{-2\eta_0})}{4(\lambda+G)} \\ & + \frac{\pi a^2P^2(\lambda+2G)}{2G(\lambda+G)}\frac{\mathrm{ch}\eta_0\mathrm{ch}2\eta_0}{\mathrm{sh}2\eta_0(\mathrm{ch}\eta_0+1)(\mathrm{ch}2\eta_0-1)} \end{aligned}$$

$$+\frac{\pi aPK(\lambda+2G)\,\mathrm{sh}\eta_0+e^{-\eta_0}}{4G(\lambda+G)\quad 1+\mathrm{ch}\eta_0}-\frac{\pi a^2P^2}{4(\lambda+G)\mathrm{sh}^2\eta_0}$$
$$+\frac{\pi aKP}{8(\lambda+G)\mathrm{sh}\eta_0}\left[\frac{\mathrm{ch}2\eta_0 e^{-\eta_0}}{\mathrm{sh}2\eta_0}+\frac{\mathrm{ch}2\eta_0}{\mathrm{ch}\eta_0}+\frac{4}{\mathrm{sh}\eta_0}S_0\right] \tag{60}$$

From this point on, the same procedure as in case I is followed. Thus, using $\lambda = 2G$ and taking the limit of E_{tot} for $\eta_0 \to \infty$ ($K \to aP_0/\mathrm{sh}^2\eta_0$, $S_0 \to 0$, $\mathrm{th}\eta_0 \to 1$) one finds

$$E_{tot} = E_0 \tag{61}$$

in excellent agreement with reality.

On the other hand, taking the limit of E_{tot} for $\eta_0 \to 0$ ($K \to 10aP_0/7\mathrm{sh}^2\eta_0$, $S_0 \to 3/4$, $\mathrm{ch}\eta_0 \to 1$, $\mathrm{sh}\eta_0 \to \eta_0$, $e^{\eta_0} \to 1$) one obtains after the algebra

$$E_{tot} = -\frac{2}{5}E_0+\frac{12}{21}E_0\frac{1}{\eta_0}+\frac{5}{12}E_0\frac{1}{\eta_0^2} \tag{62}$$

Using Equation 47 and retaining only the dominant factor of Equation 62, one ends up with

$$E_{tot} = \frac{5}{12}E_0\frac{R}{L}\cong\frac{1}{2}E_0\frac{R}{L} \tag{63}$$

Combining Equations 61 and 63, one arrives at the following expression which describes both long range and short range interaction

$$E_{tot} = E_0+\frac{1}{2}E_0\frac{R}{L} \tag{64}$$

As found in case I, the total energy increases when the holes approach, which shows that the interaction is again repulsive.

3.3. Case III: $R_2 \gg R_1$, $P_1 > P_2 = 0$

This case resembles the situation of a cylinder near a free surface [16]. Due to the considerable size difference, the curvature of the large hole can be taken as $1/R_2 \to 0$. The biharmonic Equation 9 has to be solved along with the following boundary conditions

$$\sigma_\eta(\eta_1 = \eta_0) = -P_1,\quad \sigma_\eta(\eta_2 = 0) = 0,$$
$$\sigma_{\eta\xi}(\eta_1) = \sigma_{\eta\xi}(\eta_2) = 0 \tag{65}$$

where $P = P_1$, and for no stress at infinity

$$\frac{\Phi}{J}\to 0 \quad \text{for } \eta,\ \xi \to 0 \tag{66}$$

The small hole occupies $\eta_1 = \eta_0 > 0$, where

$$\mathrm{sh}\eta_0 = \frac{a}{R} = \frac{[(L+R)^2-R^2]^{1/2}}{R} \tag{67}$$

The large hole is the curve $\eta = \eta_2 = 0$. The appropriate stress function is

$$\frac{\Phi}{J} = \frac{aP}{2\mathrm{sh}^2\eta_0}\left[\cos\xi(1-\mathrm{ch}2\eta)+\frac{\mathrm{sh}2\eta\cos\xi}{\mathrm{th}\eta_0}\right.$$
$$\left.+\frac{2\eta(\mathrm{ch}\eta-\cos\xi)}{\mathrm{th}\,\eta_0}\right] \tag{68}$$

Calculating Λ from Equations 68 and 17, one finds

$$\frac{\Lambda}{J}\frac{2(\lambda+G)}{\lambda+2G} = \frac{aP}{\mathrm{sh}^2\eta_0}\left[\frac{\mathrm{ch}2\eta\sin\xi}{\mathrm{th}\eta_0}\right.$$
$$\left.-\mathrm{sh}2\eta\sin\xi+\frac{2\xi\mathrm{ch}\eta}{\mathrm{th}\,\eta_0}\right] \tag{69}$$

Knowing Φ and Λ, the displacements u, v can be found from Equations 15 and 16. Also, the total energy can be calculated from Equation 20 as follows:

$$4GE_{tot} = \frac{-PG}{\lambda+G}\int_{-\pi}^{\pi}\left.\frac{\partial\Phi}{\partial\eta}\right|_{\eta_0}\mathrm{d}\xi$$
$$+P[\Lambda(\eta_0,\pi)-\Lambda(\eta_0,-\pi)]$$
$$= -\frac{2\pi a^2P^2}{(\lambda+G)\mathrm{sh}^3\eta_0}\left[\mathrm{sh}2\eta_0 e^{-\eta_0}\right.$$
$$-\frac{\mathrm{ch}2\eta_0-1}{2\mathrm{sh}\eta_0}-\frac{\mathrm{ch}2\eta_0 e^{-\eta_0}}{\mathrm{th}\eta_0}$$
$$\left.-\mathrm{ch}\eta_0+\frac{\mathrm{ch}\eta_0}{\mathrm{th}\eta_0}\right]$$
$$+\frac{\pi a^2P^2(\lambda+2G)\mathrm{ch}^2\eta_0}{(\lambda+G)\mathrm{sh}^3\eta_0(1+\mathrm{ch}\eta_0)} \tag{70}$$

Using $\lambda = 2G$, and taking the limit $\eta_0 \to \infty$ ($\mathrm{th}\eta_0 \to 1$) one finds

$$E_{tot} = E_0 \tag{71}$$

in perfect agreement with reality.

Taking the limit $\eta_0 \to 0$ ($\mathrm{ch}\eta_0 \to 1$, $\mathrm{sh}\eta_0 \to \eta_0$, $e^{\eta_0} \to 1$) one obtains

$$E_{tot} = \frac{2}{3}E_0+\frac{1}{3}E_0\frac{1}{\eta_0} \tag{72}$$

As seen from Equation 67, for $L/R \to 0$

$$\eta_0 \cong \left[\frac{2L}{R}\right]^{1/2} \tag{73}$$

Thus, using only the dominant factor

$$E_{tot} = \frac{1}{3\sqrt{2}}E_0\left[\frac{R}{L}\right]^{1/2}\cong\frac{1}{4}E_0\left[\frac{R}{L}\right]^{1/2} \tag{74}$$

Superimposing Equations 71 and 74, the relation for both short-range and long-range interaction is obtained

$$E_{tot} = E_0+\frac{1}{4}E_0\left[\frac{R}{L}\right]^{1/2} \tag{75}$$

Once more, the interaction is proven repulsive.

3.4. Case IV: $R_1 = R_2$, $-\sigma_2 = P_1$

In this case, the tractions on the surfaces of the two equi-sized holes are equal in magnitude but opposite in sign, i.e. one is tensile (σ_2) and the other compressive (P_1), with $|P_1| = |\sigma_2| = P$. The compressive traction represents a pressurized bubble, of course; the tensile traction represents an underpressurized bubble, i.e. a bubble for which the entrapped gas pressure is smaller than the surface tension

$$P'_2-\frac{2\gamma}{R_2}<0 \tag{76}$$

A cavity is represented by taking $P'_2 = 0$; then, due to the cavity's surface tension a tensile stress is exerted on the surrounding matrix. Thus, in the present case IV, the interaction between pressurized bubbles and cavities (or, in general, underpressurized bubbles) is examined.

The biharmonic Equation 9 has to be solved along with

$$\begin{aligned} \sigma_\eta(\eta_1 = \eta_0) &= -P \\ \sigma_{\eta\xi}(\eta_0) &= 0 \end{aligned} \tag{77}$$

and

$$\begin{aligned} \sigma_\eta(\eta_2 = -\eta_0) &= +P \\ \sigma_{\eta\xi}(-\eta_0) &= 0 \end{aligned} \tag{78}$$

With $R_1 = R_2 = R$, the two holes occupy symmetric positions as in case I, thus, η_0 is given by Equation 6. Also, for vanishing stresses at infinity

$$\frac{\Phi}{J} \to 0 \quad \text{for } \eta, \xi \to 0$$

The appropriate stress function Φ solving the biharmonic equation and satisfying the above boundary conditions is

$$\frac{\Phi}{J} = \frac{aP}{\mathrm{sh}2\eta_0(\mathrm{ch}2\eta_0 - 1)}[2\eta\mathrm{ch}2\eta_0(\mathrm{ch}\eta - \cos\xi) + \mathrm{sh}2\eta\cos\xi] \tag{79}$$

Next, Λ is calculated from Equation 17; after the algebra

$$\frac{\Lambda}{J}\frac{2(\lambda+G)}{\lambda+2G} = \frac{2aP}{\mathrm{sh}2\eta_0(\mathrm{ch}2\eta_0 - 1)}[2\xi\,\mathrm{ch}2\eta_0\mathrm{ch}\eta + \mathrm{ch}2\eta\sin\xi] \tag{80}$$

Thus, the displacements u and v can be calculated from Equations 15 and 16. The total energy will be given by the following relation:

$$E_{\mathrm{tot}} = \frac{1}{2}\int_{\mathrm{SUR}} -Pu(\eta_1)\,\mathrm{d}S + \frac{1}{2}\int_{\mathrm{SUR}} Pu(\eta_2)\,\mathrm{d}S \tag{81}$$

The above formula is similar to Equation 20 except for the plus sign indicating tensile stress in the second term of the RHS. Inserting Equations 79 and 80 into Equation 81 yields

$$\begin{aligned} 4GE_{\mathrm{tot}} = &-\frac{PG}{\lambda+G}\int_{-\pi}^{\pi}\left.\frac{\partial\Phi}{\partial\eta}\right|_{\eta_0}\mathrm{d}\xi \\ &+ P[\Lambda(\eta_0,\pi) - \Lambda(\eta_0 - \pi)] \\ &+ \frac{PG}{\lambda+G}\int_{-\pi}^{\pi}\left.\frac{\partial\Phi}{\partial\eta}\right|_{\eta_0}\mathrm{d}\xi \\ &- P[\Lambda(-\eta_0,\pi) - \Lambda(-\eta_0,-\pi)] \end{aligned} \tag{82}$$

Carrying out the integration

$$E_{\mathrm{tot}} = \frac{\pi a^2P^2}{(\lambda+G)\mathrm{sh}2\eta_0(\mathrm{ch}2\eta_0 - 1)}\left[2\mathrm{ch}2\eta_0 + \frac{2\mathrm{ch}2\eta_0 e^{-\eta_0}}{\mathrm{sh}\eta_0} - \frac{\mathrm{sh}2\eta_0}{\mathrm{sh}^2\eta_0}\right]$$

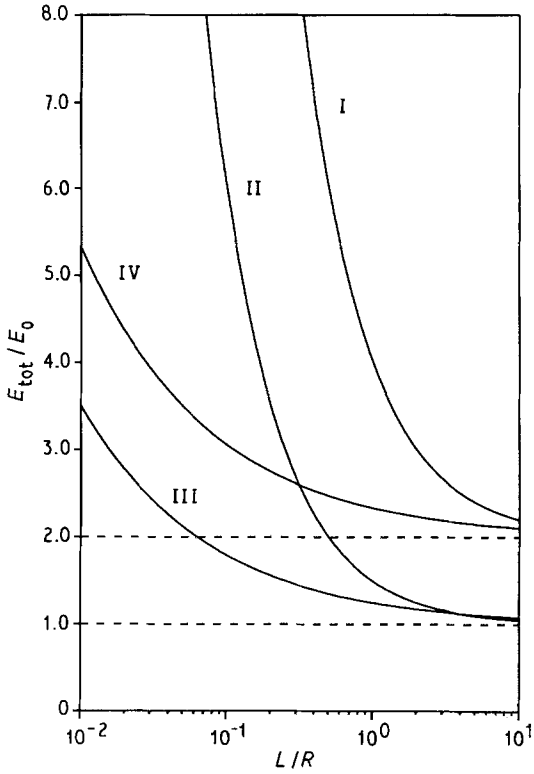

Figure 4 Ratio of the total energy E_{tot} of a system of two holes over the energy E_0 of an isolated hole of radius R and pressure P as a function of separation L, when: (I) $R_1 = R_2 = R$ and $P_1 = P_2 = P$; (II) $R_1 = R_2 = R$ and $P_1 = P$, $P_2 = 0$; (III) $R_2 \gg R_1 = R$ and $P_1 = P$, $P_2 = 0$; (IV) $R_1 = R_2 = R$ and $P_1 = P = -\sigma_2$. All four curves approach infinity for $(L/R) \to 0$.

$$+\frac{\pi a^2P^2(\lambda+2G)}{\lambda+G}\frac{\mathrm{ch}\eta_0}{1+\mathrm{ch}\eta_0}\frac{2}{\mathrm{sh}2\eta_0(\mathrm{ch}2\eta_0 - 1)}\mathrm{ch}2\eta_0 \tag{83}$$

With $\lambda = 2G$, the limit of E_{tot} for $\eta_0 \to \infty$ ($\mathrm{th}\eta_0 \to 1$) is

$$E_{\mathrm{tot}} = 2E_0 \tag{84}$$

in agreement with reality.

For $\eta_0 \to 0$ ($\mathrm{ch}\eta_0 \to 1$, $\mathrm{sh}\eta_0 \to \eta_0$, $e^{\eta_0} \to 1$)

$$E_{\mathrm{tot}} = \frac{1}{3}E_0\frac{1}{\eta_0} \tag{85}$$

For very small values of η_0, Equation 47 is valid; this gives

$$E_{\mathrm{tot}} = \frac{1}{3}E_0\left[\frac{R}{L}\right]^{1/2} \tag{86}$$

As previously, the overall interaction is obtained by superposition of the short and long range formulae

$$E_{\mathrm{tot}} = 2E_0 + \frac{1}{3}E_0\left[\frac{R}{L}\right]^{1/2} \tag{87}$$

Again, a repulsive interaction is predicted.

The results for all four cases are summarized in Fig. 4. From this figure, a general idea about how the various elastic interactions compare is also obtained.

4. Discussion

The results presented in the previous section prove

unambiguously that the elastic interactions between bubbles and cavities are always repulsive. This is exactly the opposite of what has been accepted so far; all previous models [3–5] have invariably predicted attraction in all cases.

The closed-form solutions provided for all four cases are obtained in rigorous mathematical fashion. Thus they are not based on any assumptions other than being applicable within the limits of classical elasticity. The fact that cylinders rather than spheres are analysed does not constitute any significant distortion qualitatively or quantitatively. As already mentioned in section 2, energies and stress concentrations differ only slightly (by less than a factor of 2) if at all when one compares cylinders to spheres. Thus, employing this geometrical simplification, the problem of interaction can be treated in exact mathematical terms, contrary to previous attempts which had to rely on approximate descriptions of the elastic fields around the holes. This method (of studying cylinders rather than spheres) has been successfully employed in other scientific areas, as for example for the problem of diffusive interactions and growth of bubbles and cavities.

Using the Airy stress function appropriate for each case one obtains, apart from the energies, the stresses, strains and displacements at every point. So, for instance, the displacement along η for case I is given by Equation 30. From Equations 30 and 16 one can see that the displacements at the hole surface ($\eta = \eta_0$) are not uniform but depend on ξ, i.e. change from point to point. Thus the peripheries of the holes are distorted and do not remain circular. This is an important feature of the hole-to-hole interaction. It may also be one of the reasons the predictions of previous models differ from those of the present study. So, in the works of Eshelby [3] and Lidiard and Nelson [4], the strains are taken as uniform at the holes. This is also true for the work of Willis and Bullough [5], at least for the case of interacting bubbles of significantly different sizes. For equi-sized and equi-pressurized bubbles and for large separations, the Willis and Bullough calculations coincide with the Eshelby result which, as mentioned, is derived on the basis of uniform hole deformations. However, it is apparent that the requirement of constant (normal) stress at the surfaces of interacting holes is not consistent with uniform strains and displacements at the peripheries of the holes.

As seen from Fig. 3, for small separations the elastic interaction force F_{el} (for case I) is much larger than two other natural forces, F_{gb} (force of a grain boundary on a bubble) and F_{dis} (force of a dislocation on a bubble). Thus, a bubble dragged by a grain boundary or dislocation cannot coalesce with other bubbles. The same is true for the other cases II, III and IV; as seen from Equations 64, 75 and 87 the repulsive forces are proportional to L^{-2} or $L^{-3/2}$. Thus there is always a critical distance beyond which the repulsive forces cannot be overcome. From the same Fig. 2, one can compare the elastic forces; obviously, for small separations: $F_{el}(I) > F_{el}(II) > F_{el}(IV) > F_{el}(III)$.

In all four cases, at least one of the interacting holes was a pressurized bubble. However, if one examines cavities or, in general, underpressurized bubbles in place of overpressurized ones, the results are identical. This happens because in elasticity the energies depend on the square of the stresses. So, for example, if at the surface of an isolated cavity one applies normal stress $-P$ or $+P$ the elastic energy will be identical. Similarly, the interaction between two equal cavities (underpressurized bubbles) is identical to case I; the interaction between a cavity (underpressurized bubble) and an equilibrium bubble of equal size is identical to case II; and the interaction between a cavity (underpressurized bubble) and an equilibrium bubble of much larger size is identical to case III. Hence, regardless of whether one talks about bubbles or cavities or underpressurized bubbles, the interactions are always repulsive. Preliminary numerical results (to appear in a future paper) using finite elements, are in agreement with this conclusion.

The presence of elastic repulsions constitutes a barrier to coalescence. Barnes and Mazey [1] reported experimental data where coalescence was apparently prevented by the existence of a barrier. They observed that small pressurized bubbles rotated like satellites around large equilibrium ones rather than coalescing with them.

What has been discussed so far is not meant to prove coalescence impossible. Note that repulsions develop only when at least one of the holes is either overpressurized or underpressurized. Interactions among equilibrium holes are non-existent. When elastic fields are absent, bubbles do not 'feel' the presence of other bubbles. The same thing happens in some cases where elastic fields are relaxed by atom diffusion, especially at high temperatures. In these cases the bubbles, although initially pressurized, become equilibrated by the acquisition of vacancies. Then there is no barrier to coalescence which occurs readily should the bubbles collide while moving either randomly or due to some driving force (e.g. thermal gradient).

However should any elastic fields exist, coalescence may be seriously inhibited. This can significantly restrain material swelling because, when bubbles coalesce, the volume of the new bubble is larger than the sum of the volumes of the component bubbles. Conversely, an increase in swelling is expected when elastic repulsions are relaxed. This may be one of the reasons Rest *et al.* [6] observed a significant increase in swelling rates as well as in bubble mobility and coalescence when the test material experienced a crystalline-to-amorphous transformation.

Extensive experimental work has been devoted to the phenomenon of bubble lattices [7–9, 17, 18]. Measurements show that the amount of gas entrapped in these ordered configurations is such that the individual bubbles are highly overpressurized [7] by up to a factor of 20, i.e. with internal pressure 20 times the equilibrium value. Thus, the forces between the bubbles may acquire high values since they are proportional to P^2. Elaborate models have been proposed [7, 17, 18], trying to reconcile the generally accepted idea of attraction between bubbles with the reality of the lattices. To explain the stability of these lattices, a

repulsive force is needed. Such can be provided by the elastic interactions studied here.

5. Summary and conclusions

In the preceeding sections, a complete analysis of the elastic interactions among pressurized, equilibrium and underpressurized bubbles has been presented. Using rigorous mathematical methods, the interactions have been described in terms of exact and easy-to-use formulae. It has been proven that, contrary to what has been accepted so far, all elastic interactions between holes are repulsive.

The repulsive force has been found to increase in magnitude when the holes approach. Quantitative comparisons with experiments are hindered by the unavailability of detailed measurements of the strength of the interactions; this is unfortunate, in view of the simplicity of the derived formulae which permit almost any combination of pressures, separations and bubble radii to be treated readily. However, experimental observations where coalescence is inhibited by a barrier are in agreement with the predicted repulsions. Furthermore, such repulsive interactions may constitute the 'missing link' for the explanation of the commonly observed bubble lattices.

Finally the elastic repulsions, with their role as coalescence inhibitors, may considerably decrease the swelling of materials.

References

1. R. S. BARNES and D. J. MAZEY, *Proc. R. Soc.* **275A** (1963) 47.
2. F. A. NICHOLS, *J. Nucl. Mater.* **30** (1969) 143.
3. J. D. ESHELBY, *Annalen der Physik* **1** (1958) 116.
4. A. B. LIDIARD and R. S. NELSON, *Phil. Mag.* **17** (1968) 425.
5. J. R. WILLIS and R. BULLOUGH, *J. Nucl. Mater.* **32** (1969) 76.
6. J. REST, G. L. HOFMAN and R. C. BIRCHEN, in Proceedings of the 14th International Symposium on the Effects of Radiation on Materials, Vol. 2, edited by N. H. Packan, R. E. Stoller and A. S. Kumar (ASTM, 1990).
7. K. KRISHAN, *Rad. Eff.* **66** (1982) 121.
8. P. B. JOHNSON and D. J. MAZEY, *Nature* **276** (1978) 595.
9. P. B. JOHNSON, A. L. MALCOLM and D. J. MAZEY, *ibid.* **329** (1987) 310.
10. S. P. TIMOSHENKO, "Theory of Elasticity" (McGraw-Hill, New York, 1951).
11. A. E. H. LOVE, "Mathematical Theory of Elasticity" (Cambridge University Press, New York, 1927).
12. E. STERNBERG and M. A. SADOWSKY, *J. Appl. Mech.* **19** (1952) 19.
13. E. TSUCHIDA, I. NAKAHARA and M. KODAMA, *Bull. JSME* **19** (1976) 993.
14. C.-B. LING, *J. Appl. Phys.* **19** (1948) 77.
15. G. B. JEFFERY, *Phil. Trans.* **221A** (1921) 265.
16. G. N. SAVIN, "Stress Concentrations Around Holes" (Pergamon, London, 1961).
17. V. I. DUBINKO, V. V. SLEZOV, A.V. TUR and V. V. YANOVSKIJ, *Rad. Eff.* **100** (1986) 85.
18. V. I. DUBINKO, A.V. TUR, A. V. TURKIN and V. V. YANOVSKIJ, *J. Nucl. Mater.* **161** (1989) 57.

Received 21 November 1990
and accepted 10 April 1991